# Supplementary Information

# *Elp2* mutations perturb the epitranscriptome and lead to a complex neurodevelopmental phenotype

**Kojic *et al*.**

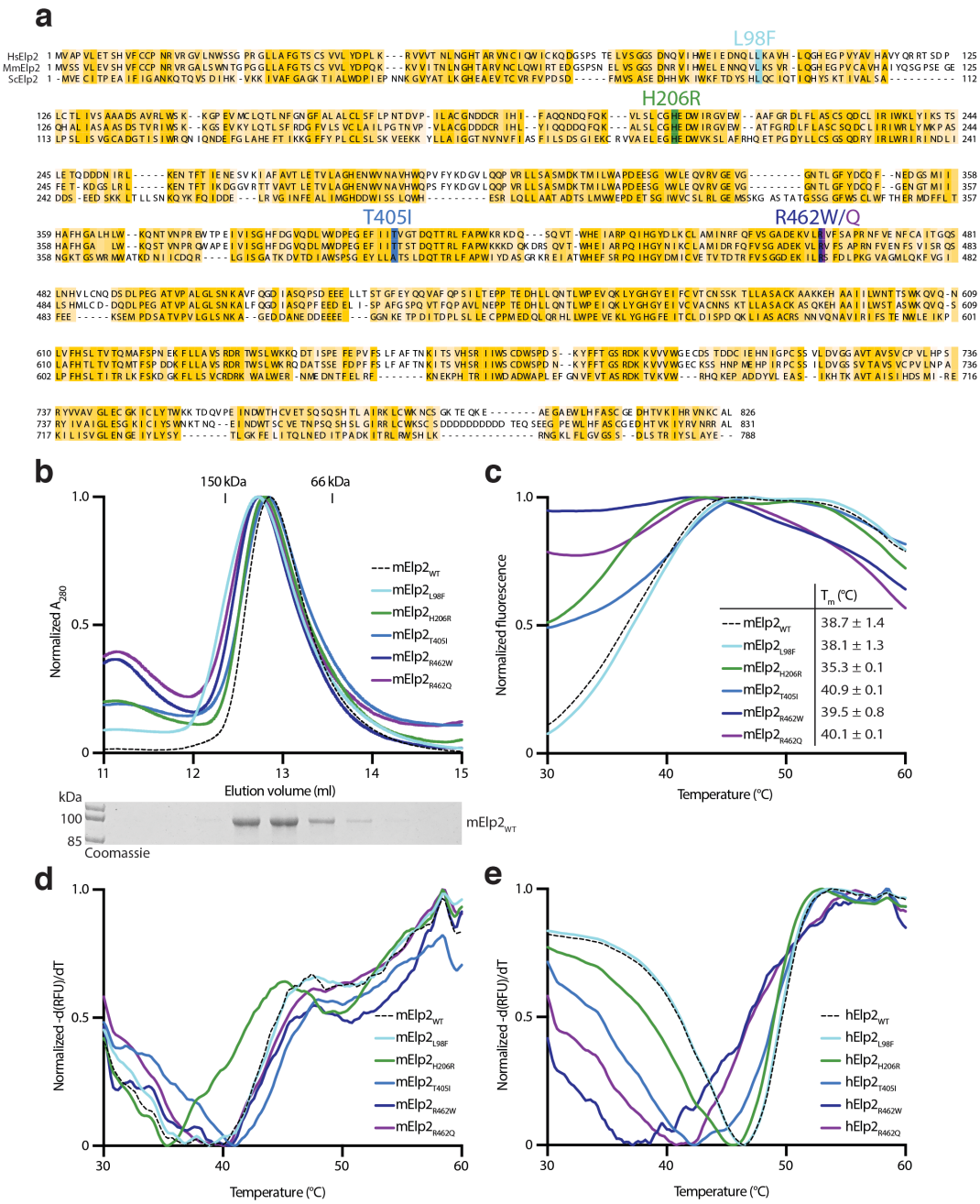


**Supplementary Figure 1. Mutations found in patients with intellectual disability and autism impair the mElp2 protein stability.** (**a**) Alignment of *Homo sapiens* (HsElp2), *Mus musculus* (MmElp2), *Saccharomyces cerevisiae* (ScElp2) Elp2 protein sequences with highlighted location of patient-derived mutations. Residues are labelled in orange depending on the conservation score. (**b**) Purification of mouse Elp2 wild-type ($mElp2_{WT}$) and mutant proteins ($mElp2_{L98F}$, $mElp2_{H206R}$, $mElp2_{T405I}$, $mElp2_{R462W}$, $mElp2_{R462Q}$). Gel filtration profiles from S200 Increase 10/300 GL column for mElp2 variants (top) and Coomassie-stained SDS-PAGE gel for $mElp2_{WT}$ (bottom). $n = 3$ independent experiments. (**c**) Averaged melting curves from thermal shift assay for mElp2 variants with calculated melting temperatures ($T_m$) (mean ± SD). (**d**) Normalized first derivative plot from thermal shift assay experiments for mElp2 variants. (**e**) Normalized first derivative plot from thermal shift assay experiments for hElp2 variants. $n = 3$ independent measurements for (**c-e**). Source data are provided as a Source Data file.

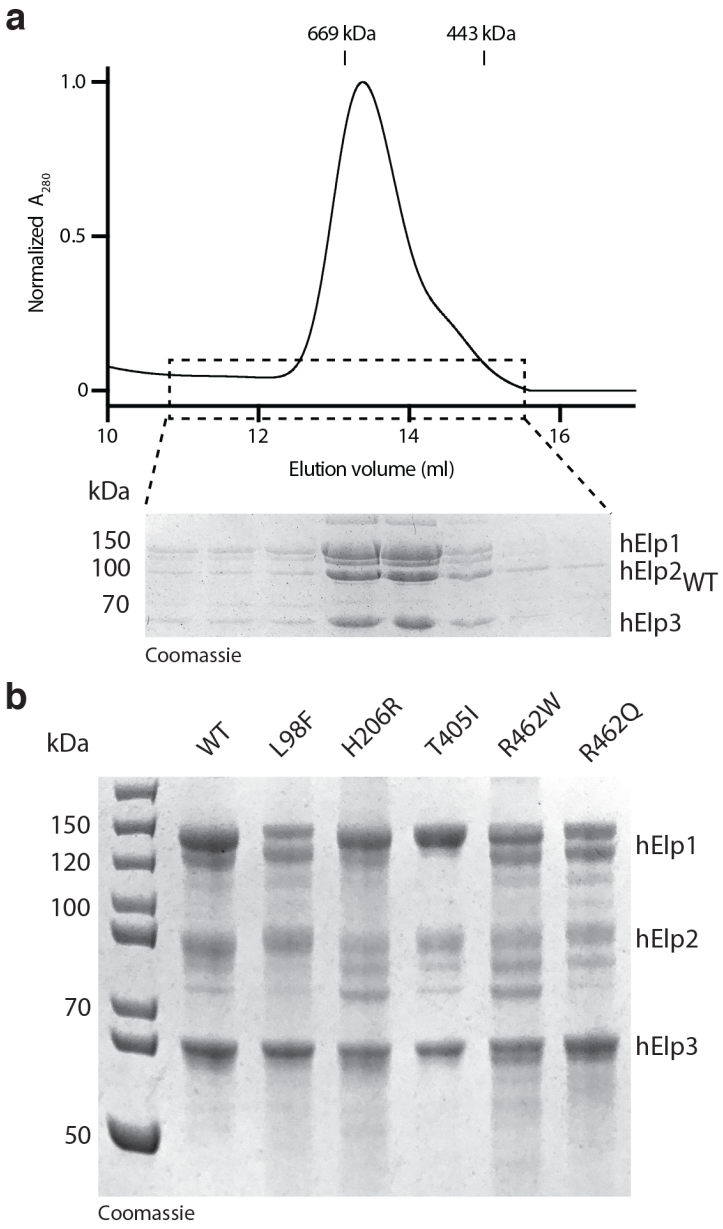


**Supplementary Figure 2. Purified hElp123 subcomplex variants**. (**a**) Gel filtration profile from Superose 6 Increase 10/300 GL column for hElp123 (top) and SDS PAGE of the respective fractions stained with Coomassie (bottom). (**b**) Coomassie-stained SDS-PAGE gel of purified human Elp123 wild-type (hElp123$_{WT}$) and mutant variants (hElp2$_{L98F}$3, hElp2$_{H206R}$3, hElp2$_{T405I}$3, hElp2$_{R462W}$3, hElp2$_{R462Q}$3) with hElp123 subunits marked on the right side of the gel. $n$ = 3 independent experiments for both (**a**) and (**b**). Source data are provided as a Source Data file.

**a**

| Genotype | 9-10 dpc Expected | 9-10 dpc Observed | 14-15 dpc Expected | 14-15 dpc Observed | 16-17 dpc Expected | 16-17 dpc Observed | 18-18.5 dpc Expected | 18-18.5 dpc Observed | Weaned Expected | Weaned Observed |
|---|---|---|---|---|---|---|---|---|---|---|
| *Elp2* $^{+/+}$ | 10.5 | 17 | 9 | 11 | 6.25 | 9 | | | 14.25 | 19 |
| *Elp2* $^{H206R/+}$ | 10.5 | 10 | 9 | 7 | 6.25 | 10 | | | 14.25 | 16 |
| *Elp2* $^{+/-}$ | 10.5 | 9 | 9 | 13 | 6.25 | 6 | Not analyzed | | 14.25 | 22 |
| ***Elp2*** $^{H206R/-}$ | 10.5 | 6 | 9 | 5 | 6.25 | 0 | | | 14.25 | 0 |
| Total | 42 | | 36 | | 25 | | | | 57 | |
| *Elp2* $^{+/+}$ | 11.75 | 15 | 8 | 7 | | | | | 15.25 | 18 |
| *Elp2* $^{R464W/+}$ | 11.75 | 9 | 8 | 12 | | | | | 15.25 | 28 |
| *Elp2* $^{+/-}$ | 11.75 | 17 | 8 | 13 | Not analyzed | | Not analyzed | | 15.25 | 15 |
| ***Elp2*** $^{R464W/-}$ | 11.75 | 6 | 8 | 0 | | | | | 15.25 | 0 |
| Total | 47 | | 32 | | | | | | 61 | |
| *Elp2* $^{+/+}$ | 9.5 | 7 | 8.25 | 7 | 10.5 | 14 | 6.5 | 10 | 21 | 23 |
| *Elp2* $^{H206R/+}$ | 9.5 | 11 | 8.25 | 9 | 10.5 | 9 | 6.5 | 5 | 21 | 32 |
| *Elp2* $^{R464W/+}$ | 9.5 | 12 | 8.25 | 6 | 10.5 | 13 | 6.5 | 8 | 21 | 29 |
| ***Elp2*** $^{H206R/R464W}$ | 9.5 | 8 | 8.25 | 11 | 10.5 | 6 | 6.5 | 3 | 21 | 0 |
| Total | 38 | | 33 | | 42 | | 26 | | 84 | |
| *Elp2* $^{+/+}$ | 11.5 | 23 | 9.5 | 10 | | | | | 18 | 29 |
| *Elp2* $^{R464W/+}$ | 23 | 29 | 19 | 28 | | | | | 36 | 43 |
| ***Elp2*** $^{R464W/R464W}$ | 11.5 | 7 | 9.5 | 0 | Not analyzed | | Not analyzed | | 18 | 0 |
| Total | 46 | | 38 | | | | | | 72 | |

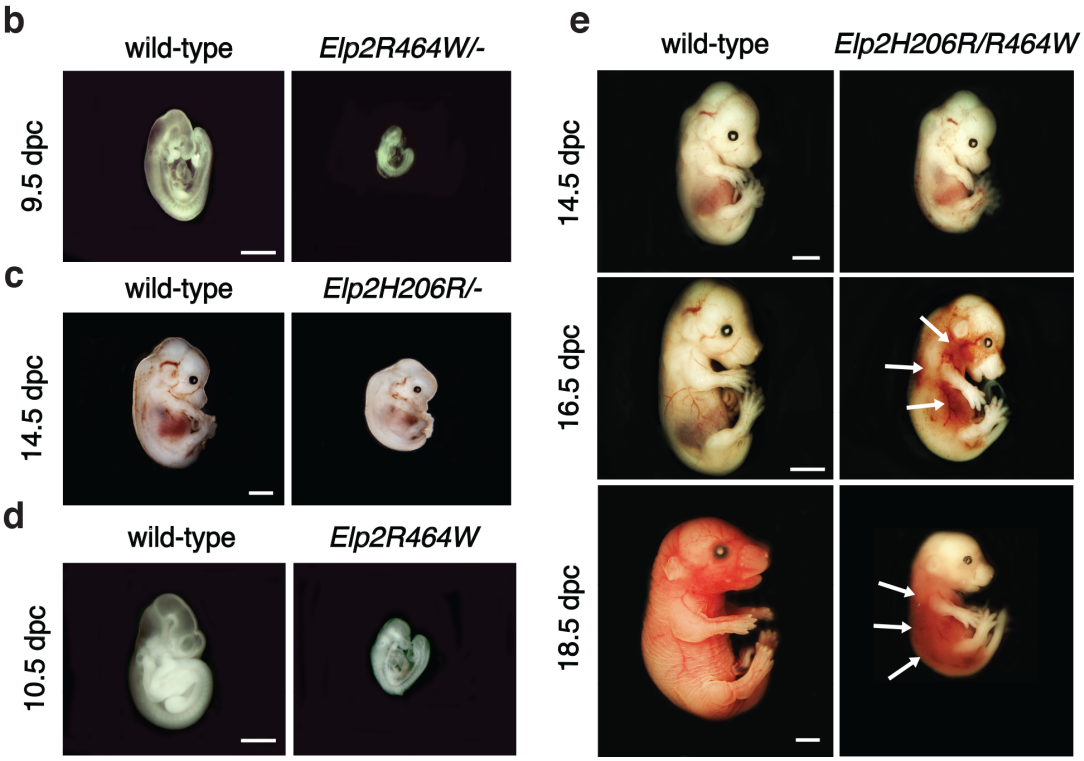


**Supplementary Figure 3. Embryonic lethality of *Elp2* mutations on C57BL/6 genetic background.** (**a**) Expected and observed genotypes based on Mendelian frequency from *Elp2*$^{H206R/+}$ and *Elp2*$^{+/-}$ (first row), *Elp2*$^{R464W/+}$ and *Elp2*$^{+/-}$ (second row), *Elp2*$^{H206R/+}$ and *Elp2*$^{R464W/+}$ (third row), and *Elp2*$^{R464W/+}$ (last row) intercrosses at different stages of development. Representative whole-mount images are shown for: (**b**) compound heterozygous embryos for *Elp2R464W* and *Elp2* null mutation (*Elp2R464W*/-), (**c**) compound heterozygotes for *Elp2H206R* and *Elp2* null mutation (*Elp2H206R*/-), (**d**) *Elp2R464W* homozygous (*Elp2R464W*) and (**e**) compound heterozygous embryos for *Elp2R464W* and *Elp2H206R* mutations (*Elp2H206R*/*R464W*), and matching littermate controls for each genotype at indicated stages of the embryonic development. Arrows point to haemorrhaging in the mutant embryos. Number of embryos per genotype is indicated in (**a**); representative images are shown (**b**-**e**). Scale bars, 1 mm. Abbreviations: dpc - days post-coitum.

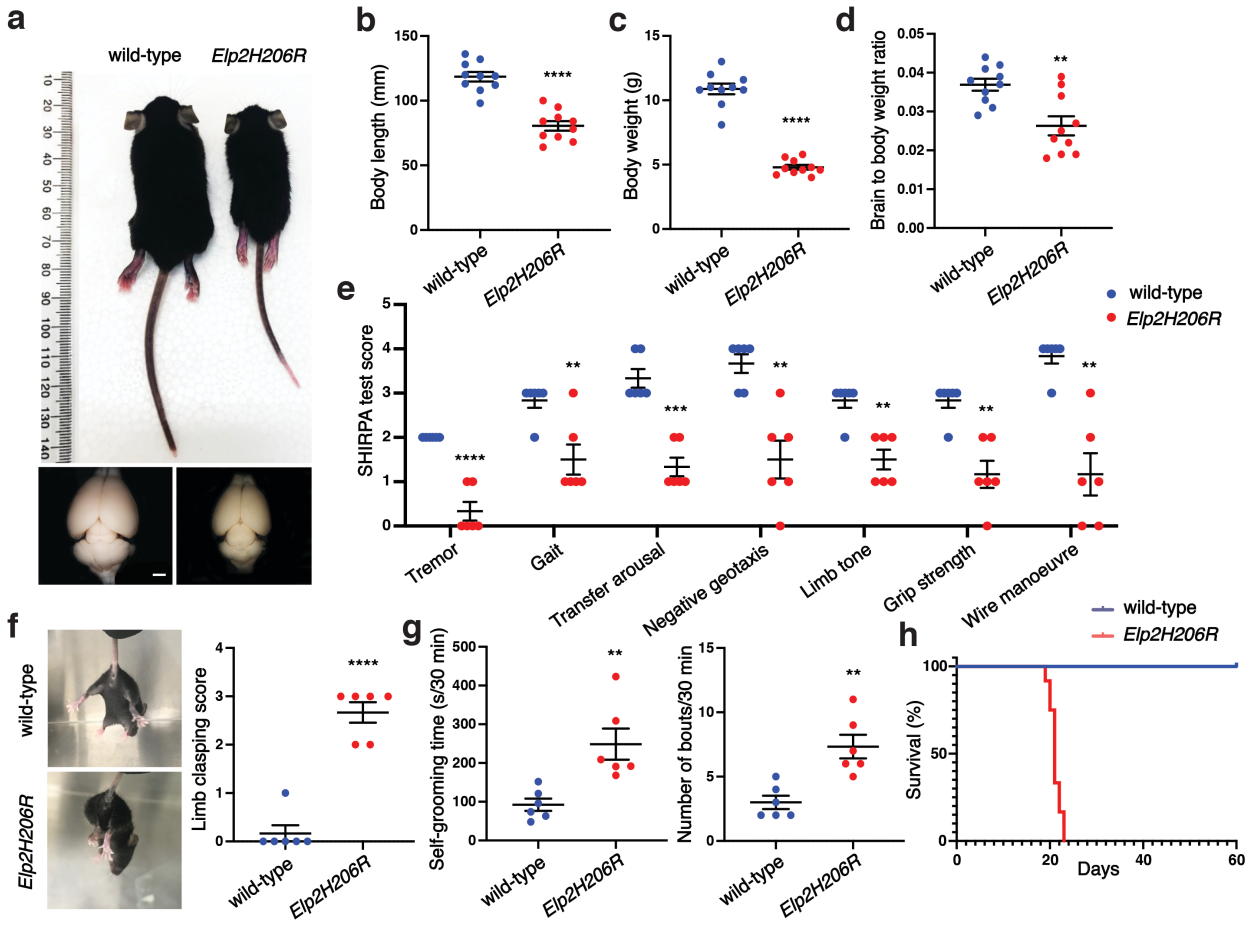


**Supplementary Figure 4. *Elp2H206R* mice show signs of developmental delay, microcephaly, motor and autism-like defects.** (**a**) Appearance of an *Elp2H206R* homozygous mouse on C57BL/6 genetic background and its control littermate (upper panel), as well as their dissected brains (lower panel; scale bar, 2 mm) at postnatal day 21 (P21). (**b**) Body length, (**c**) weight and (**d**) relative brain weight of the indicated genotypes were quantified at P21. (**e**) Significant effects of *Elp2H206R* on scores for SHIRPA test at P21. (**f**) Representative image (left) and scoring (right) of hindlimb clasping in P21 wild-type and mutant mice. (**g**) Total self-grooming time and number of self-grooming bouts in *Elp2H206R* mutants vs. control at P21 (recorded for 30 min in a home cage). For (**a-d**) $n = 10$ (5 males and 5 females) and for (**e-g**) $n = 6$ (3 males and 3 females). (**h**) Kaplan–Meier curve of mouse survival ($n = 12$). Statistical analysis: unpaired two-tailed *t*-test ($\alpha = 0.05$) with Welch's correction. Holm-Sidak correction was applied to adjust for multiple comparisons (**e**). Statistically significant differences are indicated (**$p \leq 0.01$; ***$p \leq 0.001$; ****$p \leq 0.0001$). Data represent mean ± SEM. Source data are provided as a Source Data file.

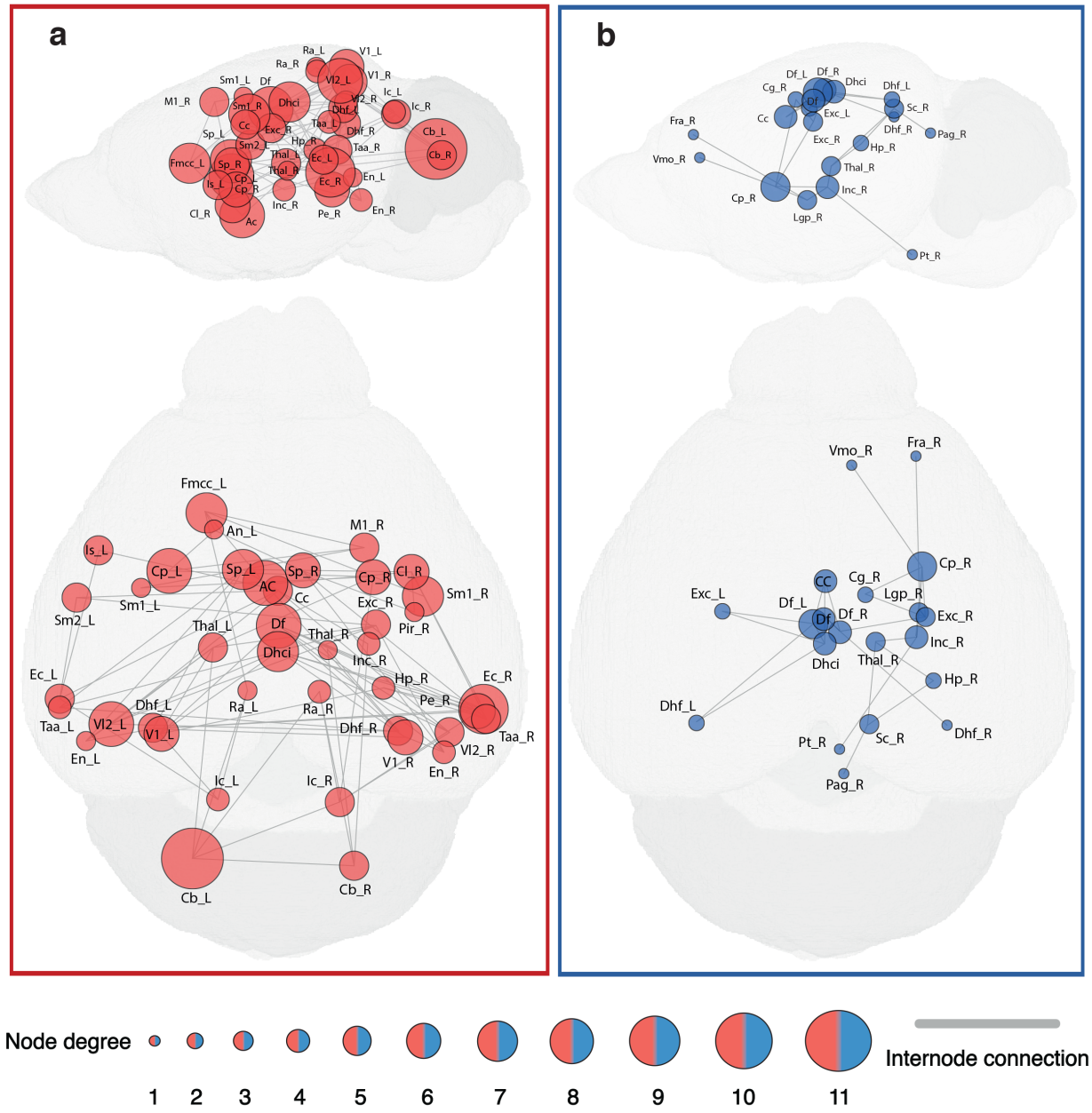


**Supplementary Figure 5. Altered brain connectivity in *Elp2H206R* mice.** Structural connectome maps generated via whole brain white matter tractography showing (**a**) increased and (**b**) decreased connectivity in *Elp2H206R* homozygous mice in comparison to their wild-type littermates *(n* = 6 animals per genotype) at postnatal day 21-23. Specific structures (nodes) within the brain are represented as circles, scaled according to the number of abnormal connections associated with that node (node degree). The maps are presented in sagittal (upper panels) and axial (lower panels) planes. Nodes exhibiting decreased connectivity in the brains of *Elp2H206R* mice are depicted in blue, while nodes with increased connectivity are shown in red. Nodes with a degree higher than 2 are included in the increased connectivity network for visualization purposes. Abbreviations: Ac - anterior commissure, An - accumbens nucleus, Cb - cerebellum, Cc - corpus callosum, Cc/Exc - corpus callosum/external capsule, Cg - cingulum, Cl - claustrum, Cp - caudate putamen, Df - dorsal fornix, Dhci - dorsal hippocampal commissure inclusion, Dhf - dorsal hippocampal fissure, Ec - ectorhinal cortex, En - entorhinal cortex, Fmcc - forceps minor of the corpus callosum, Fra - frontal association cortex, Hp - hippocampus, Ic - inferior colliculus, Inc - internal capsule, Is - insular cortex, L – left, Lgp - lateral globus pallidus, M1 - primary motor cortex, Pag - periaqueductal grey, Pe - perirhinal cortex, Pir - piriform nucleus, Pt - pyramidal tract, R – right, Ra - retrosplenial area, Sc - superior colliculus, Sm1 - primary somatosensory cortex, Sm2 - secondary somatosensory cortex, Sp - septum, Taa - temporal association area, Thal - thalamus, V1 - primary visual cortex, Vl2 – secondary visual cortex (lateral), Vmo - ventromedial orbital cortex.

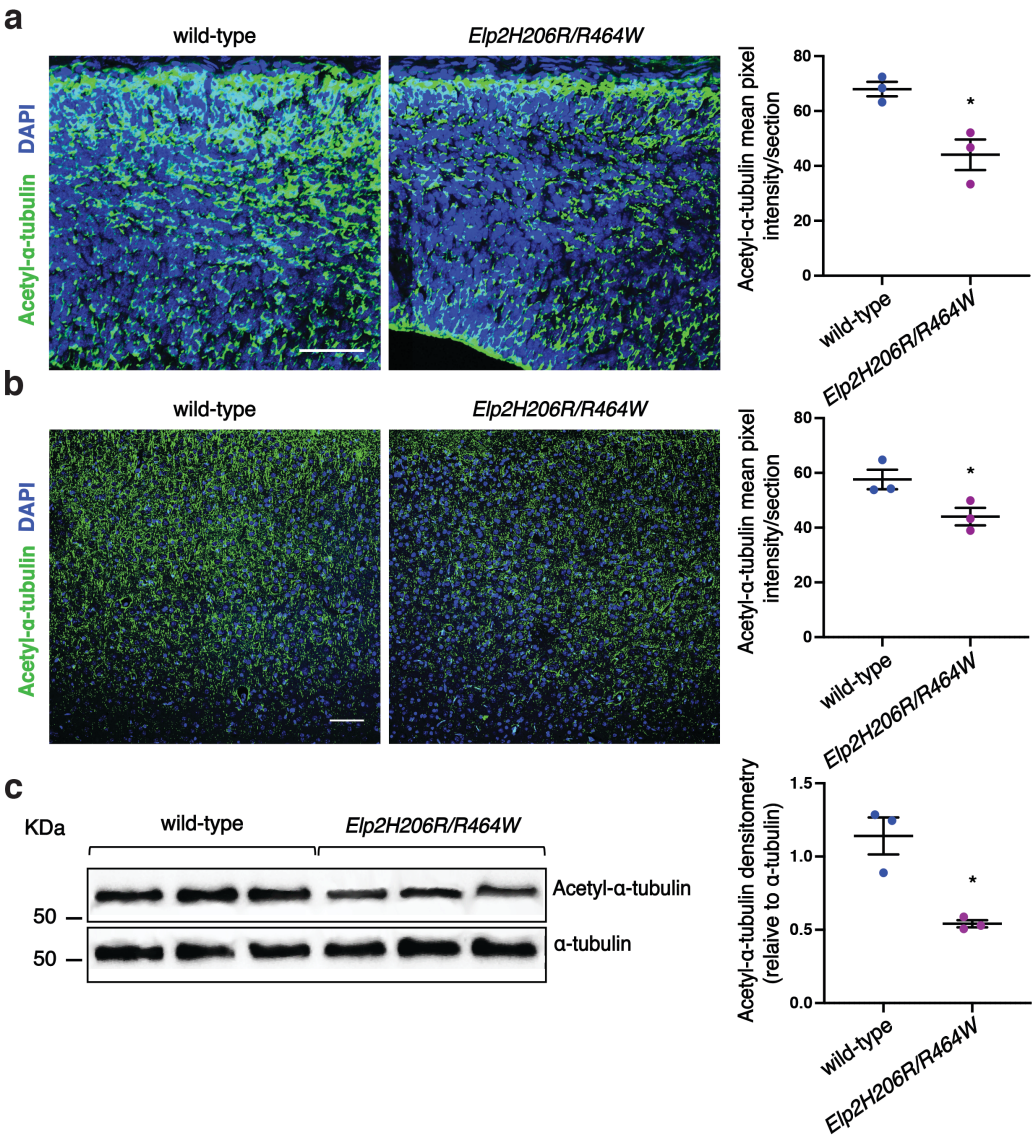


**Supplementary Figure 6. Acetylation defects in the brain cortex of *Elp2* mutant mice.** (**a**) Acetyl-α-tubulin immunostaining and mean pixel intensity quantification on coronal brain sections of 14.5 days post-coitum and (**b**) adult (2-months-old) wild-type and *Elp2H206R/R464W* mice. Sections were counterstained with DAPI. (**c**) Quantification of acetyl-α-tubulin expression relative to α-tubulin in adult brains by western blot. $n = 3$ animals per genotype and 3 sections per animal (**a** and **b**); representative images are shown. Scale bars, 100 µm. Statistical analysis: unpaired two-tailed *t*-test ($\alpha = 0.05$) with Welch's correction. Statistically significant differences are indicated (*$p \leq 0.05$: for (**a**) $p = 0.0329$; for (**b**) $p = 0.0483$; for (**c**) $p = 0.0373$). Data represent mean ± SEM. Source data are provided as a Source Data file.

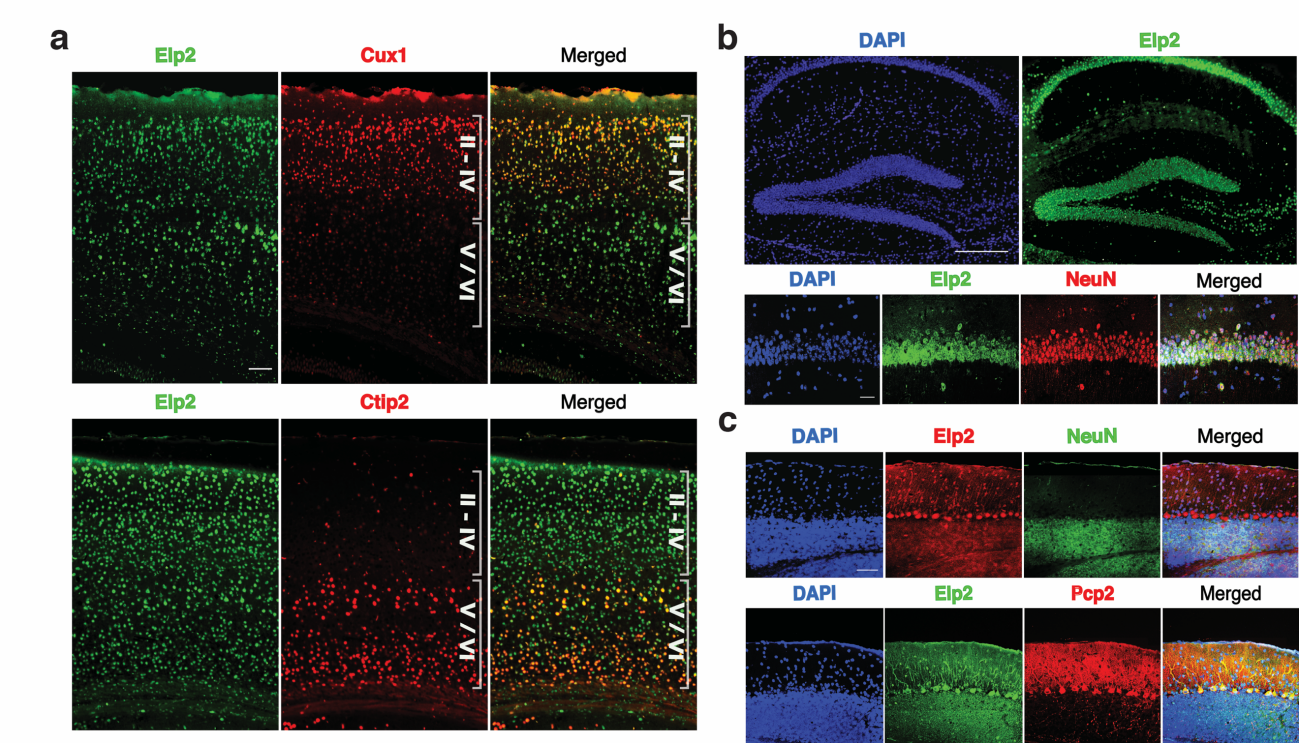


**Supplementary Figure 7. Elp2 is expressed by cortical, hippocampal and cerebellar neurons.** Immunolabelling of brain sections of adult (2-months-old) wild-type mice showing Elp2 expression in (**a**) upper (II-IV; Cux1-labelled neurons) and lower (V/VI; Ctip2-labelled neurons) cortical layers, (**b**) hippocampal neurons (marked by NeuN) and (**c**) granule (NeuN-labelled) and Purkinje neurons (Pcp2-labelled) in the cerebellum. Sections were counterstained with DAPI. *n* = 3 animals and 3 sections per animal; representative images are shown. Scale bars, 100 µm (**a**), 200 µm (**b** upper panels) and 50 µm (**b** lower panels and **c**).

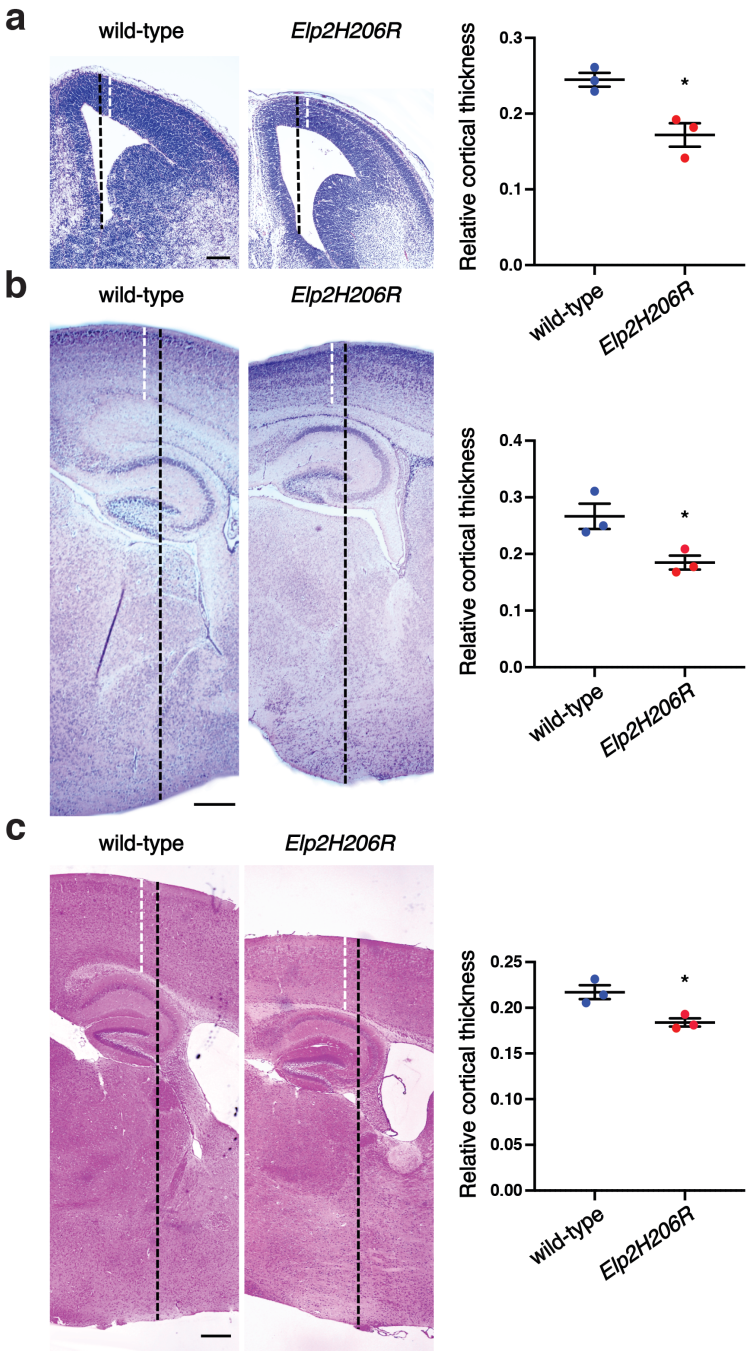


**Supplementary Figure 8. Reduced cortical thickness in *Elp2H206R* mice.** (**a**) H&E-stained brain sections of 14.5 days post-coitum embryos (coronal sections), (**b**) 7-days-old and (**c**) adult (2-months-old; sagittal sections) *Elp2H206R* and wild-type mice. Thicknesses of the cortical layers (white lines) were quantified relative to the section thicknesses indicated by black lines. $n = 3$ animals per genotype and 3 sections per animal; representative images are shown. Scale bars, 100 µm (**a**) and 500 µm (**b** and **c**). Statistical analysis: unpaired two-tailed *t*-test ($\alpha = 0.05$) with Welch's correction. Statistically significant differences are indicated (*$p \leq 0.05$: for (**a**) $p = 0.0234$; for (**b**) $p = 0.0471$: for (**c**) $p = 0.0288$). Data represent mean ± SEM. Source data are provided as a Source Data file.

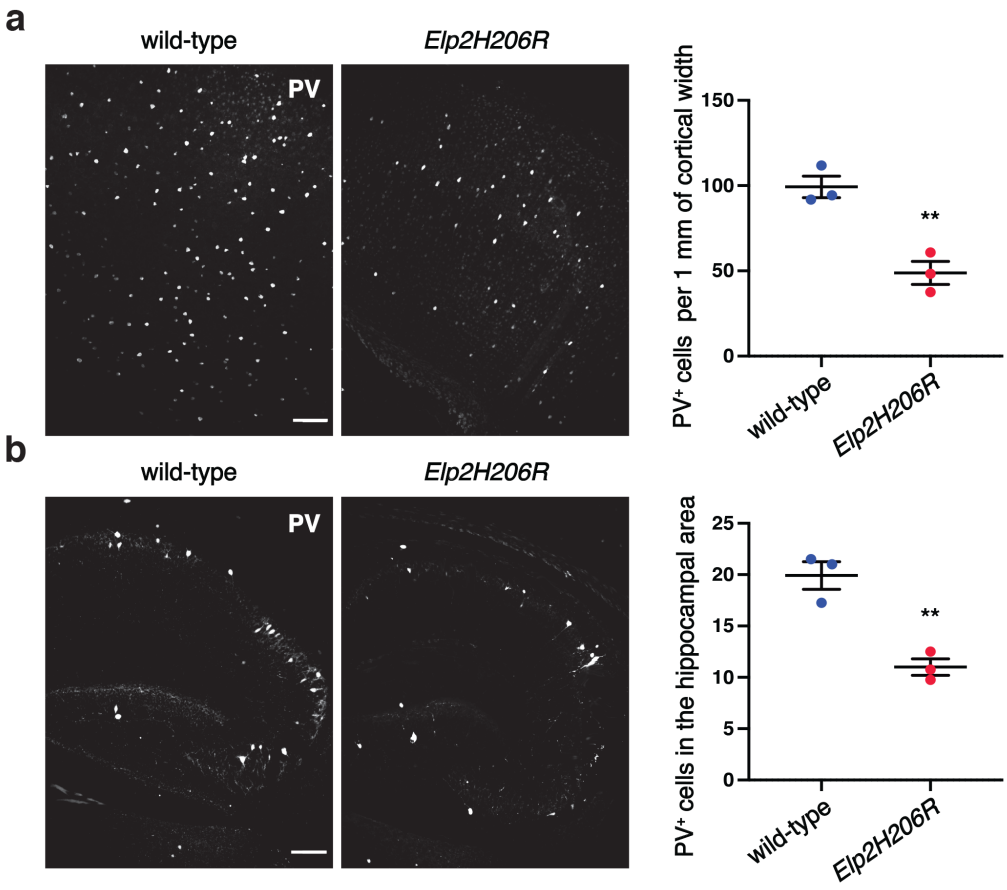


**Supplementary Figure 9. Interneuron defects in *Elp2H206R* mice.** (**a**) Immunofluorescence labelling and quantification of cortical and (**b**) hippocampal parvalbumin (PV)-expressing interneurons in adult (2-months-old) brains of *Elp2H206R* mice and their wild-type littermates. $n = 3$ animals per genotype and 4 sections per animal; representative images are shown. Scale bars, 100 µm. Statistical analysis: unpaired two-tailed *t*-test ($\alpha = 0.05$) with Welch's correction. Statistically significant differences are indicated (**$p \leq 0.01$: for (**a**) $p = 0.0055$: for (**b**) $p = 0.0084$). Data represent mean ± SEM. Source data are provided as a Source Data file.

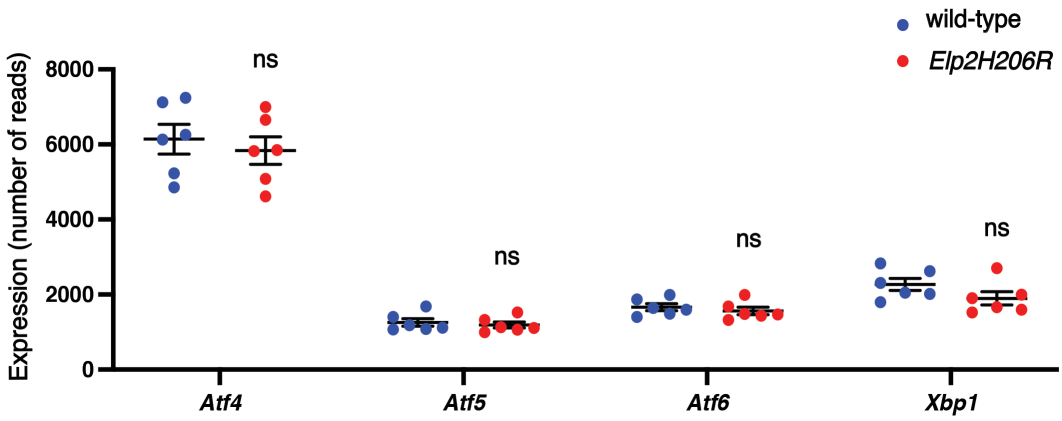


**Supplementary Figure 10. Expression of unfolded protein response genes in the developing brain of *Elp2H206R* mice.** Transcriptomic analysis of the key genes involved in the unfolded protein response, namely *Atf4* and *Atf5* (PERK pathway), *Atf6* and *Xbp1* (IRE-1α pathway) in the forebrain extracts of *Elp2H206R* vs. wild-type 14.5 days post-coitum embryos ($n$ = 6 animals per genotype). Statistical analysis: unpaired two-tailed $t$-test ($\alpha$ = 0.05). Holm-Sidak correction was applied to adjust for multiple comparisons. Statistically significant differences are indicated (ns - not significant: $p$ = 0.7053 for *Atf4*; $p$ = 0.9346 for both *Atf5* and *Atf6*; $p$ = 0.6539 for *Xbp1*). Source data are provided as a Source Data file.

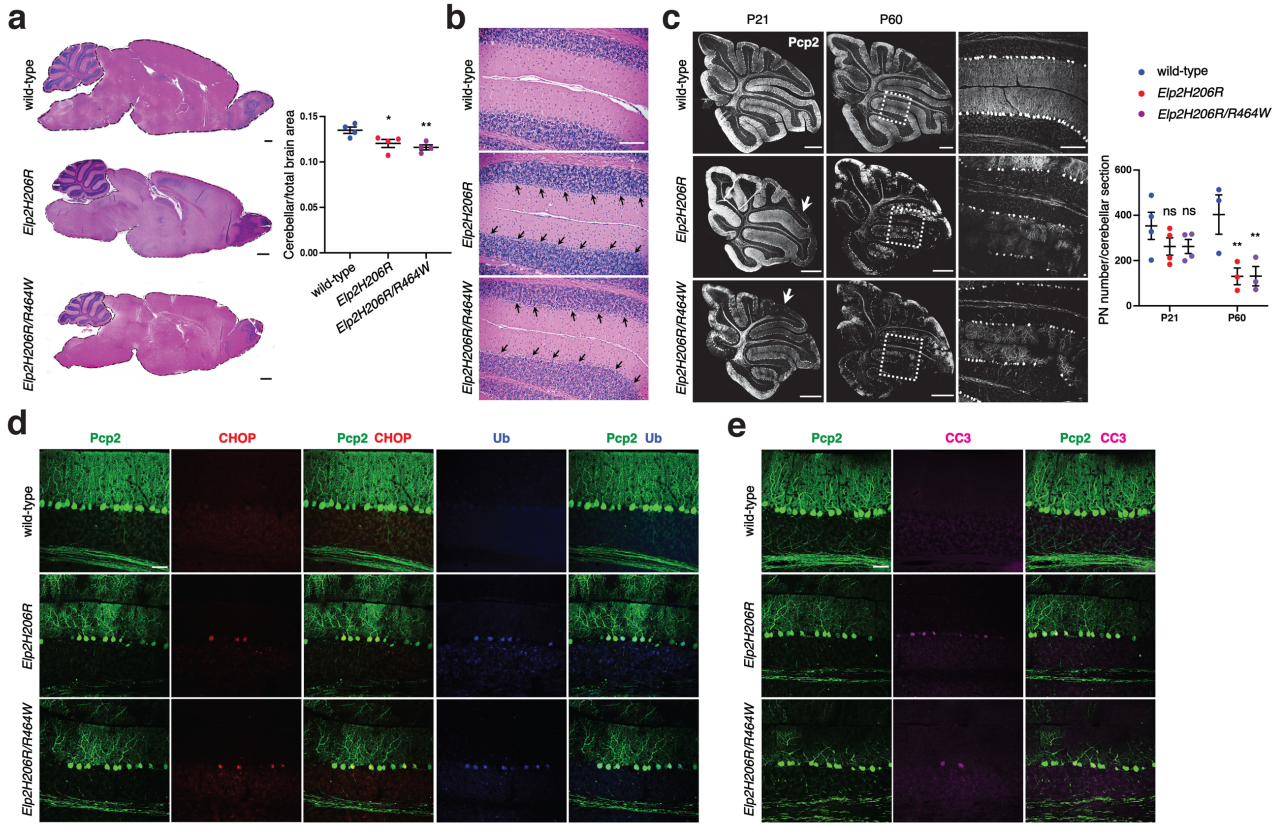


**Supplementary Figure 11. Protein misfolding and ER-stress-induced apoptosis in Purkinje neurons in *Elp2* mutant mice.** (**a**) H&E-stained sagittal brain sections of wild-type, *Elp2H206R* homozygous and *Elp2H206R*/*R464W* compound heterozygous mice at postnatal day 60 (P60). Cerebellar area relative to the whole-brain area was quantified (marked by dashed line). (**b**) Magnified cerebellar lobules from (**a**). Arrows indicate Purkinje neuron (PN) loss. (**c**) Pcp2 immunofluorescence and PN quantification in *Elp2* mutant and control mice at P21 and P60. Arrows indicate PN loss and white rectangles represent magnified areas. (**d**) Immunofluorescence staining of P60 cerebellar sections for expression of CHOP, ubiquitin (Ub) and (**e**) cleaved caspase-3 (CC3) in Purkinje neurons (Pcp2). For (**a**), (**b**) and (**c**) at P21 $n = 4$ mice per genotype, for (**c**) at P60, (**d**) and (**e**) $n = 3$ animals per genotype and 3 sections per animal; representative images are shown. Scale bars, 500 µm (**a** and **c** left and middle panels), 100 µm (**b** and **c** right panels) and 50 µm (**d** and **e**). Statistical analysis: one-way ANOVA ($\alpha = 0.05$) (**a**) and two-way ANOVA ($\alpha = 0.05$) (**c**) with a Dunnett's post-hoc test. Statistically significant differences are indicated (*$p \leq 0.05$: $p = 0.0356$; **$p \leq 0.01$: for (**a**) $p = 0.0094$; for (**c**) $p = 0.0061$ for *Elp2H206R* and $p = 0.0062$ for *Elp2H206R*/*R464W*; ns - not significant: $p = 0.3254$ for *Elp2H206R* and $p = 0.3266$ for *Elp2H206R*/*R464W*). Data represent mean ± SEM. Source data are provided as a Source Data file.

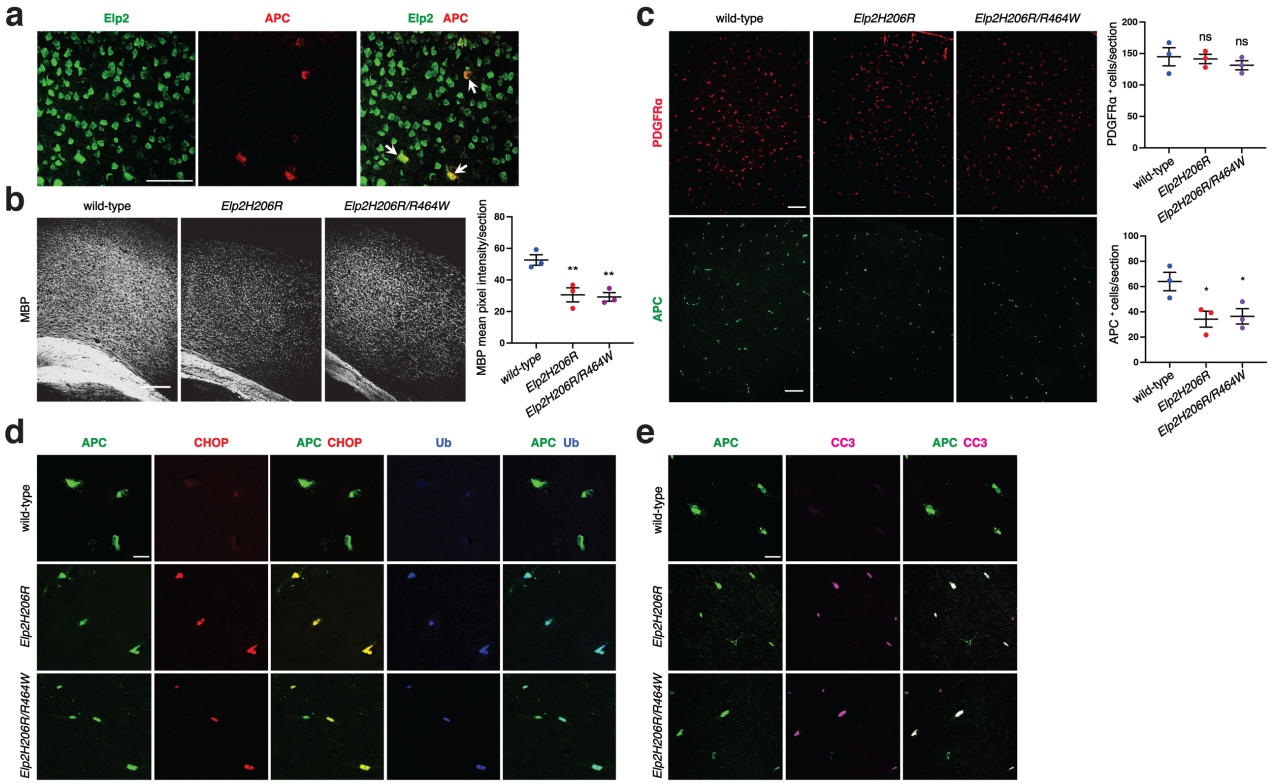


**Supplementary Figure 12. Unfolded protein response-mediated myelin destruction in the brain of *Elp2* mutant mice.** (**a**) Immunolabelling of brain sections of adult (2-months-old) wild-type mice showing Elp2 expression in oligodendrocytes (APC-labelled). (**b**) Myelin basic protein (MBP) immunostaining on sagittal brain sections of adult wild-type, *Elp2H206R* homozygous and *Elp2H206R/R464W* compound heterozygous mice, and mean pixel intensity quantification. (**c**) Immunostaining and quantification of oligodendrocyte progenitor cells (PDGFRα-labelled) and mature oligodendrocytes (APC) in the brain of wild-type and the *Elp2* mutant animals. (**d**) Immunofluorescence staining of cortical sections for CHOP, ubiquitin (Ub) and (**e**) cleaved caspase-3 (CC3) expression in oligodendrocytes (APC). $n = 3$ animals per genotype and 3 sections per animal; representative images are shown. Scale bars, 100 µm (**a** and **c**), 500 µm (**b**) and 20 µm (**d** and **e**). Statistical analysis: one-way ANOVA ($\alpha = 0.05$) with a Dunnett's post-hoc test. Statistically significant differences are indicated (*$p \leq 0.05$: $p = 0.033$ for *Elp2H206R* and $p = 0.0445$ for *Elp2H206R/R464W*; **$p \leq 0.01$: $p = 0.0086$ for *Elp2H206R* and $p = 0.0065$ for *Elp2H206R/R464W*; ns - not significant: $p = 0.9575$ for *Elp2H206R* and $p = 0.5774$ for *Elp2H206R/R464W*). Data represent mean ± SEM. Source data are provided as a Source Data file.

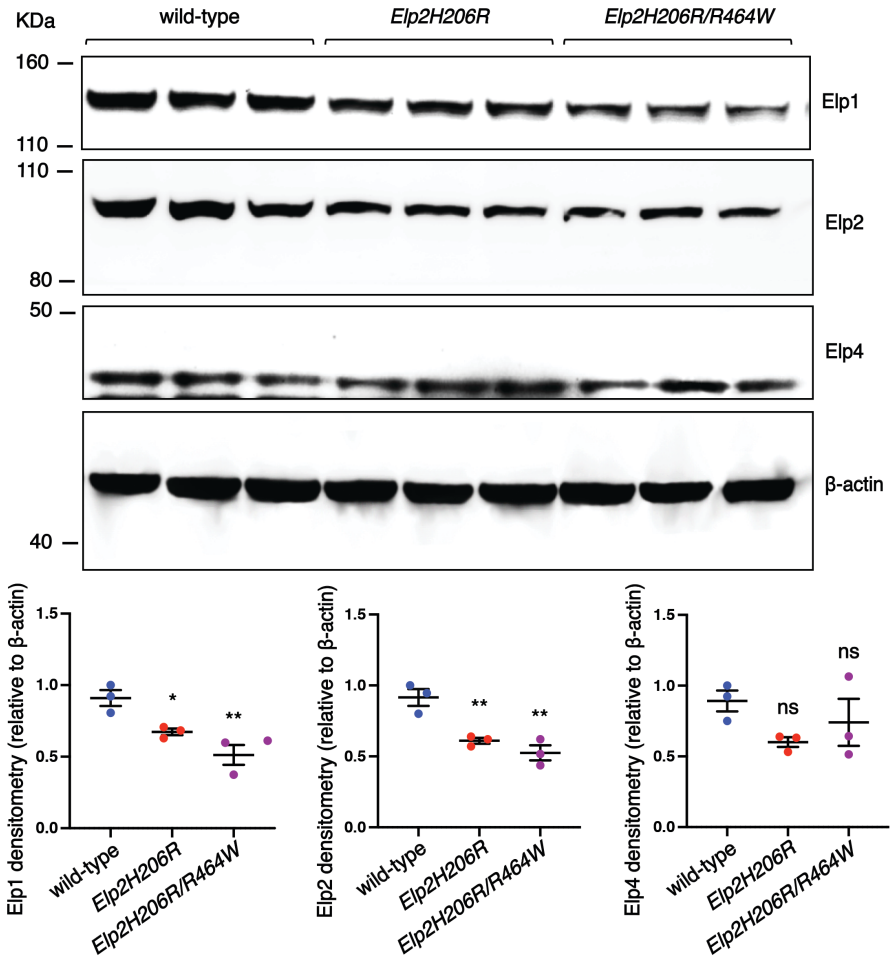


**Supplementary Figure 13. Expression of Elongator subunits in the brain tissue of *Elp2* mutant mice.** Western blot analysis of Elp1, Elp2 and Elp4 expression in the brain lysates of adult (2-months-old) wild-type, *Elp2H206R* and *Elp2H206R*/*R464W* mice. The levels of expression were quantified and normalized with β-actin. $n$ = 3 animals per genotype. Statistical analysis: one-way ANOVA ($\alpha$ = 0.05) with a Dunnett's post-hoc test. Statistically significant differences are indicated (*$p \leq 0.05$: $p = 0.0353$; **$p \leq 0.01$: for Elp1 densitometry $p = 0.0034$; for Elp2 densitometry $p = 0.0071$ for *Elp2H206R* and $p = 0.0021$ for *Elp2H206R*/*R464W*; ns - not significant: $p = 0.1724$ for *Elp2H206R* and $p = 0.5383$ for *Elp2H206R*/*R464W*). Data represent mean ± SEM. Source data are provided as a Source Data file.

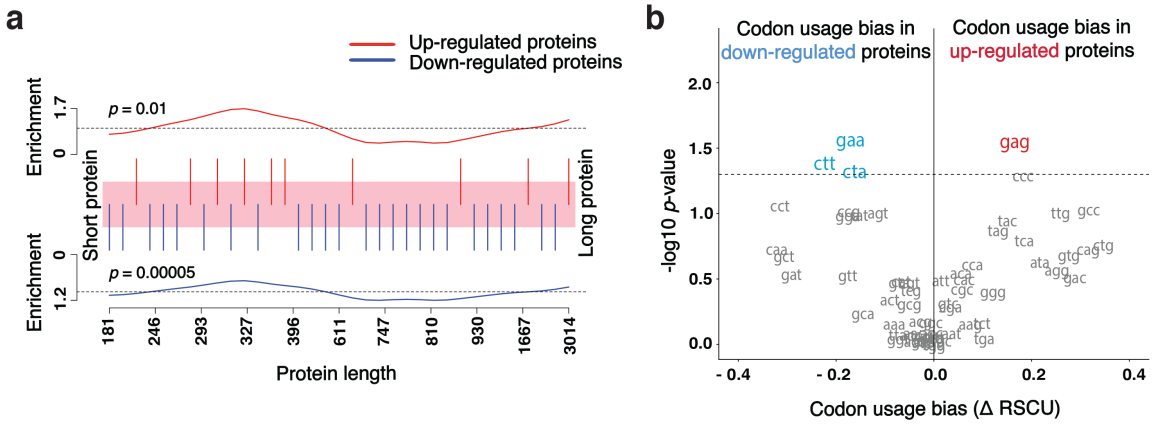


**Supplementary Figure 14. Protein length and codon usage in developing brains of *Elp2H206R* vs. control mice.** (**a**) Length distribution among up- and down-regulated proteins in the cortical extracts of *Elp2H206R* vs. wild-type 14.5 days post-coitum embryos. (**b**) Codon usage bias (AA-ending vs. AG-ending codons) in down- and up-regulated proteins. *n* = 3 animals per genotype. Statistical analysis: Wilcoxon test. Statistically significant differences are indicated in the image. Source data are provided as a Source Data file.

**Supplementary Table 1. Main clinical features of patients carrying disease-causing *ELP2* variants**

| | Patient 1 (Cohen et al, 2015) | Patient 2 (Cohen et al, 2015) | Patient 3 | Patient 4 | Patient 5 | Patient 6 | Patient 7 | Patient 8 |
|---|---|---|---|---|---|---|---|---|
| ***ELP2* variants** | p. H206R + p. R462W | p. H206R + p. R462W | p. L98Ffs*10 + p. T405I | p. L98Ffs*10 + p. T405I | p. H206R + p. N506Kfs*8 | p. R462Q + p. Q553* | p. L444S + p. R820Sfs*3 | p. R462Q (homozygous) |
| **Sex, age** | Male, 30 y | Male, deceased: 25 y (accidental choking) | Male, 18 m | Female, deceased: 4,5 m (respiratory insufficiency) | Male, 29 m | Male, 17 y, 9 m | Female, 25 y | Male, 17 y, 3 m |
| **Prenatal/neonatal course** | Hypotonia | Uncomplicated | Hypotonia, asphyxia, breathing difficulty, progressing heart insufficiency | Hypotonia, asphyxia, breathing difficulty, progressing heart insufficiency, oedema | Hypotonia | Uncomplicated | Uncomplicated | Uncomplicated |
| **Developmental delay** | Severe - profound | Severe - profound | Severe - profound | Unable to evaluate | Severe | Severe - profound | Unable to evaluate (most likely severe) | Severe - profound |
| **Intellectual disability** | Severe | Severe | NA | NA | NA | Profound | Severe | Severe |
| **Age of sitting/ walking** | 14 m/9 y, later lost the ability to walk | 15 m/never achieved | Never achieved | Never achieved | 18 m/not yet walking | Never achieved | Unknown | 10 m/never achieved |
| **Language abilities** | ~ 50 words, lost meaningful spoken language | Non-verbal | Non-verbal | Non-verbal | Non-verbal | Non-verbal | 4-5 y | Non-verbal |
| **Use of hands** | Purposeful hand use | Purposeful hand use | No targeted movements, poor grasping function | Uncoordinated movements | Purposeful hand use, clumsy, poor pincer grasp, stereotypies | Stereotypies: hand rubbing and wringing | Purposeful hand use | Stereotypies: hand wringing and flapping |
| **Behaviour/ASD** | Severe self-injury/ ASD | Severe self-injury/ ASD | Excessive sleepiness | Excessive sleepiness | ASD | Shaking/laughing episodes | Aggressivity/ASD | Self-stimulatory behabiour, hyperactive/ASD |
| **Feeding difficulty** | No | No | Yes, PEG-tube since 10 m, reflux | Yes, PEG-tube since 5m | Yes, PEG-tube since 23 m | Yes, PEG-tube | No | Yes |
| **Neurological exam** | Truncal hypotonia, spastic diplegia, choreoathetosis, ataxia | Truncal hypotonia, spastic diplegia, choreoathetosis | Truncal hypotonia, spastic paraplegia | Dystonia | Truncal hypotonia, spastic diplegia | Spastic tetraplegia | Normal | Hypotonia of extremities, paroxysmal generalized dystonia |
| **Ophtamological features** | Normal vision | Normal vision | CVI, unilateral coloboma | Poor eye contact, bilateral colobomas | CVI, foveal hypoplasia, nystagmus, dysconjugate gaze, exophoria | Normal vision, nystagmus | Normal vision | CVI, nystagmus |
| **Epilepsy** | No | No | Yes | Suspected, not confirmed | No | Yes | Yes | Yes |
| **Age of onset/ seizure type** | NA | NA | 9 m/IS, SE | NA | NA | 17 y, 9m/GTCS, SE | 14 y/GTCS | 4 y, 9m/nocturnal GTCS |
| **EEG** | Normal | Normal | Modified hypsarrhythmia | Normal | Mild diffuse slowing | Normal | Waves of generalized polyspikes | Moderate diffuse slowing |
| **AED received** | NR | NR | VGB, LEV, ZNS, HD | NR | NR | LEV | VPA, ZNS, LEV, PB | NR |
| **Seizure frequency** | NA | NA | Weekly | NA | NA | Unknown | Weekly | Monthly |
| **Brain MRI or UL** | Normal | Normal | UL: general atrophy, bilateral cysts in surrounding lateral ventricles | MRI: general atrophy, subependymale pseudocysts | UL: choroid plexus cyst - disappeared before birth MRI: delayed but improving myelination, thin corpus callosum | MRI: profound cerebellar, brainstem and supratentorial cortical atrophy, WM volume loss with secondary ventriculomegaly and increased extra-axial CSF spaces, microcephaly | Normal | MRI: simplified gyral pattern, cortical atrophy, white matter atrophy |
| **Congenital malformations/ additional features** | None | None | VSD, ASD*, PDA/ renal hypoplasia | VSD, ASD*, PDA/ broncho- and tracheomalacia, rectal prolapse, umbilical hernia | None/stridor, larygomalacia from 1 m, sleep apnea | None | None | None |

Abbreviations: AED – antiepileptic drugs, ASD - autism spectrum disorder, ASD* - atrial septal defect, CVI - cortical visual impairment, DD - developmental delay, EEG – electroencephalography, GTCS - generalized tonic-clonic seizure, HD - hydrocortisone, ID - intellectual disability; IS - infantile spasms, LEV - levetiracetam, m - months, MRI - magnetic resonance imaging, NA – not applicable, NR – not required, PB - phenobarbital, PDA - patent ductus arteriosus, PEG - percutaneous endoscopic gastrostomy, SE - status epilepticus, UL - ultrasound, VGB - vigabatrin, VPA - valproic acid, VSD - ventricular septal defect, y - years, ZNS – zonisamide.

**Supplementary Table 2. Volume changes in the *Elp2H206R* mouse brain**

| | Relative change in the volume of mouse brain regions (% of the total brain volume; mean ± SEM) | | |
|---|---|---|---|
| **Structure** | **wild-type** | ***Elp2H206R*** | **Adjusted p-value** |
| Hippocampus | 5.867633 ± 0.065787 | 6.354618 ± 0.111298 | 0.050803 |
| External capsule | 3.093557 ± 0.102202 | 2.672847 ± 0.145684 | 0.308714 |
| Caudate putamen | 5.933934 ± 0.061846 | 6.024996 ± 0.073479 | 0.846351 |
| Anterior Commisure | 0.201652 ± 0.002974 | 0.2597788 ± 0.014108 | 0.017915 |
| Globus Pallidus | 0.543824 ± 0.028228 | 0.4389170 ± 0.018203 | 0.223214 |
| Internal Capsule | 0.422742 ± 0.021723 | 0.2353112 ± 0.010209 | 0.002993 |
| Thalamus | 6.399709 ± 0.093350 | 5.894091 ± 0.081598 | 0.061725 |
| Cerebellum | 11.941060 ± 0.181416 | 10.61362 ± 0.314935 | 0.054305 |
| Superior Colliculi | 2.080718 ± 0.058053 | 2.119778 ± 0.093725 | 0.609423 |
| Ventricles | 0.247034 ± 0.008119 | 0.3528514 ± 0.02239 | 0.950982 |
| Hypothalamus | 3.082076 ± 0.065848 | 4.383420 ± 0.172950 | 0.000761 |
| Inferior Colliculi | 1.337301 ± 0.054331 | 1.455590 ± 0.060843 | 0.723786 |
| Central gray | 1.164943 ± 0.029093 | 1.248244 ± 0.085077 | 0.840945 |
| Neocortex | 33.282940 ± 0.303790 | 31.33459 ± 0.230353 | 0.025144 |
| Amygdala | 2.362849 ± 0.058855 | 2.705513 ± 0.113525 | 0.184297 |
| Olfactory Bulb | 5.578876 ± 0.178943 | 5.677643 ± 0.497516 | 0.950982 |
| Brain stem | 10.247510 ± 0.186211 | 10.89033 ± 0.35135 | 0.571517 |
| Rest of Midbrain | 2.760917 ± 0.039672 | 2.891464 ± 0.056690 | 0.515425 |
| Basal Forebrain Septum | 2.918191 ± 0.071703 | 3.926801 ± 0.132316 | 0.001559 |
| Fimbria | 0.532533 ± 0.015699 | 0.5195933 ± 0.021863 | 0.950982 |

Sample registration to the BNL C57BL/6J adult mouse brain atlas enabled model-based segmentation and volumetric measurement of listed brain structures in *Elp2H206R* homozygous mice and their wild-type littermates ($n = 6$) at postnatal day 21-23. Statistically significant differences are shown in red. Statistical analysis: two-tailed *t*-test with Holm-Sidak correction.

**Supplementary Table 3. Increased connectivity in *Elp2H206R* mouse brain**

| Node | Node degree | Node | Node degree |
|---|---|---|---|
| Cerebellum L | 11 | Subiculum R | 2 |
| Ectorhinal cortex R | 9 | Secondary motor cortex R | 2 |
| Secondary visual cortex lateral L | 8 | Ventromedial orbital cortex L | 2 |
| Caudate putamen L | 8 | Secondary somatosensory cortex R | 2 |
| Anterior commissure | 8 | Secondary visual cortex mediolateral R | 2 |
| Dorsal fornix | 8 | Insular cortex R | 2 |
| Primary somatosensory cortex R | 7 | Perirhinal cortex L | 2 |
| Septum L | 7 | Claustrum L | 2 |
| Forceps minor of the cospus callosum L | 7 | Endopiriform nucleus L | 2 |
| Dorsal hippocampal commisure inclusion | 7 | Piriform nucleus L | 2 |
| Primary visual cortex L | 6 | Amygdala L | 2 |
| Primary visual cortex R | 6 | Amygdala R | 2 |
| Perirhinal cortex R | 6 | Hippocampus L | 2 |
| Clustrum R | 6 | Cingulum R | 2 |
| Caudate putamen R | 6 | Dorsal fornix L | 2 |
| Septum R | 6 | Lateral olfactory tract L | 2 |
| Primary motor cortex R | 5 | Pyramidal tract L | 2 |
| Secondary somatosensory cortex L | 5 | Pyramidal tract R | 2 |
| Temporal association area R | 5 | Fornix | 2 |
| Secondary visual cortex lateral R | 5 | Dorsolateral orbital cortex R | 1 |
| Insular cortex L | 5 | Frontal cortex, area 3 R | 1 |
| Ectorhinal cortex L | 5 | Frontal association cortex L | 1 |
| Thalamus L | 5 | Lateral orbital cortex R | 1 |
| Inferior colliculus L | 5 | Primary motor cortex L | 1 |
| Cerebellum R | 5 | Secondary motor cortex L | 1 |
| Dorsal hippocampal fissure L | 5 | Endopiriform nucleus R | 1 |
| Dorsal hippocampal fissure R | 5 | Lateral globus pallidus L | 1 |
| Corpus callosum (inside midline) | 5 | Hypothalamus L | 1 |
| Corpus callosum/external capsule R | 5 | Hypothalamus R | 1 |
| Entorhinal cortex R | 4 | Superior colliculus R | 1 |
| Temporal association area L | 4 | Dorsal fornix R | 1 |
| Retrosplenial area R | 4 | Lateral olfactory tract R | 1 |
| Hippocampus R | 4 | Internal capsule L | 1 |
| Inferior colliculus L | 4 | Hindbrain L | 1 |
| Internal capsule R | 4 | | |
| Subiculum L | 3 | | |
| Entorhinal cortex L | 3 | | |
| Frontal association cortex R | 3 | | |
| Primary somatosensory cortex L | 3 | | |
| Secondary auditory cortex R | 3 | | |
| ANterior cingulate L | 3 | | |
| Retrosplenial area L | 3 | | |
| Piriform nucleus R | 3 | | |
| Accumbens nucleus L | 3 | | |
| Thalamus R | 3 | | |
| Cingulum L | 3 | | |
| Forceps minor of the corpus callosum R | 3 | | |
| Ventral hippocampal commisure inclusion | 3 | | |
| Corpus callosum/external capsule L | 3 | | |

Structural connectome generated via whole brain white matter tractography of wild-type and *Elp2H206R* homozygous mice ($n$ = 6 per genotype) at postnatal day 21-23. Increased connectivity in listed brain structures (nodes) in *Elp2H206R* mice is relative to their wild-type littermates. Node degree represents the number of abnormal connections associated with the node. Abbreviations: L - left, R - right.

**Supplementary Table 4. Decreased connectivity in *Elp2H206R* mouse brain**

| Node | Node degree |
|---|---|
| Caudate putamen R | 5 |
| Dorsal fornix L | 5 |
| Dorsal fornix R | 4 |
| Internal capsule R | 4 |
| Dorsal hippocampal commisure inclusion | 4 |
| Dorsal fornix | 4 |
| Corpus callosum (inside midline) | 4 |
| Lateral globus pallidus R | 3 |
| Thalamus R | 3 |
| Superior colliculus R | 3 |
| Corpus callosum/external capsule R | 3 |
| Hippocampus R | 2 |
| Cingulum R | 2 |
| Dorsal hippocampal fissure L | 2 |
| Corpus callosum/external capsule L | 2 |
| Frontal association cortex R | 1 |
| Ventromedial orbital cortex R | 1 |
| Periaqueductal grey R | 1 |
| Dorsal hippocampal fissure R | 1 |
| Pyramidal tract R | 1 |

Structural connectome generated via whole brain white matter tractography of wild-type and *Elp2H206R* homozygous mice ($n$ = 6 per genotype) at postnatal day 21-23. Decreased connectivity in listed brain structures (nodes) in *Elp2H206R* mice is relative to their wild-type littermates. Node degree represents the number of abnormal connections associated with the node. Abbreviations: L - left, R - right.

**Supplementary Table 5. Sequences of primers used in this study**

| Primer | Sequence 5'- 3' |
|---|---|
| Elp2H206R_for and Elp2KO_for (genotyping) | CGAGTGCCTTACAGCATACCCGC |
| Elp2H206R_for and Elp2KO_rev (genotyping) | AACCTGCTTCTCACCCCACAGTGC |
| Elp2R464W_for (genotyping) | TTCAGGGCCTTCCTTCCACTTGA |
| Elp2R464W_rev (genotyping) | TGCTGTTTTAGAGTCTTGAACTCATTTG |
| hElp2_L98F_for | GAAATCGAGGATAACCAGCTGTTCAAAGCTGTTCACCTGCAGG |
| hElp2_L98F_rev | CCTGCAGGTGAACAGCTTTGAACAGCTGGTTATCCTCGATTTC |
| hElp2_H206R_for | GTTCTGAGCCTGTGCGGTCGCGAAGATTGGATCCGTG |
| hElp2_H206R_rev | CACGGATCCAATCTTCGCGACCGCACAGGCTCAGAAC |
| hElp2_T405I_for | GGAAGGCGAGTTCATCATCATCGTTGGCACCGACCAGACC |
| hElp2_T405I_rev | GGTCTGGTCGGTGCCAACGATGATGATGAACTCGCCTTCC |
| hElp2_R464W_for | CTGATGAAAAAGTTCTGTGGGTGTTCAGCGCGCCG |
| hElp2_R464W_rev | CGGCGCGCTGAACACCCACAGAACTTTTTCATCAG |
| hElp2_R464Q_for | CTGATGAAAAAGTTCTGTCAATGTTCAGCGCGCCG |
| hElp2_R464Q_rev | CGGCGCGCTGAACACTTGCAGAACTTTTTCATCAG |
| mElp2_L98F_for | GAACTAGAGAATAATCAGGTTTTTAAATCAGTCCGTCTCCAAGGCC |
| mElp2_L98F_rev | GGCCTTGGAGACGGACTGATTTAAAAACCTGATTATTCTCTAGTTC |
| mElp2_H206R_for | CTTTCTCTCTGCGGACGCGAGGACTGGATAAGAG |
| mElp2_H206R_rev | CTCTTATCCAGTCCTCGCGTCCGCAGAGAGAAAG |
| mElp2_T404I_for | CAGAGGGAGAGTTCATCATCATTACCAGCACCGATCAGACCAC |
| mElp2_T404I_rev | GTGGTCTGATCGGTGCTGGTAATGATGATGAACTCTCCCTCTG |
| mElp2_R464W_for | GCAGACGAGAAAGTTCTTTGGGTTTTTTCTGCTCCTCGG |
| mElp2_R464W_rev | CCGAGGAGCAGAAAAAACCCAAAGAACTTTCTCGTCTGC |
| mElp2_R464Q_for | GCAGACGAGAAAGTTCTTCAAGTTTTTTCTGCTCCTCGG |
| mElp2_R464Q_rev | CCGAGGAGCAGAAAAAACTTGAAGAACTTTCTCGTCTGC |

Abbreviations: for – forward, rev – reverse.